

3 Coherence Properties of the Electromagnetic Field

3.1 Correlation Functions

The single mode electric field can be written as

$$E(r, t) = E_0 u(r) a e^{-i\omega t} + E_0 u^*(r) a^+ e^{i\omega t} \quad (92)$$

$$\equiv E^{(+)} + E^{(-)} \quad (93)$$

where $u(r)$ is the mode function (including polarization), a and a^+ are annihilation and creation operators (or c-numbers in a classical field), and E_0 is the electric field per photon.

The probability to detect a photon with a photon detector is proportional to

$$P_{fi} = |\langle f | E^+(r, t) | i \rangle|^2 \quad (94)$$

where $\langle i |$ and $\langle f |$ are initial and final field states. Only the part of the electric field which has annihilation operators is "sandwiched" between the states (the reason for this will be discussed in a later chapter).

A summation over all possible final states yields:

$$I(r, t) = \sum_f P_{fi} = \sum_f \langle i | E^-(r, t) | f \rangle \langle f | E^+(r, t) | i \rangle = \langle i | E^-(r, t) E^+(r, t) | i \rangle \quad (95)$$

If the field is initially not in a pure but in a mixed state this expression can be generalized to:

$$I(r, t) = \sum_i p_i \langle i | E^-(r, t) E^+(r, t) | i \rangle \quad (96)$$

$$= Tr \{ \rho E^-(r, t) E^+(r, t) \} \quad (97)$$

with the density operator

$$\rho = \sum_{i,j} p_{i,j} |i\rangle \langle j| \quad (98)$$

Obviously

$$\langle 0 | E^-(r, t) E^+(r, t) | 0 \rangle = 0 \quad (99)$$

The expression above is an example for a correlation function. It is the *first order correlation* or *first order coherence function*:

$$G^{(1)}(x, x') = Tr \{ \rho E^-(x) E^+(x') \} \quad (100)$$

where $x = (r, t)$, $x' = (r', t')$.

It can be generalized to the n -th order correlation or n -th order coherence function:

$$G^{(n)}(x_1, x_2, \dots, x_n, x'_1, x'_2, \dots, x'_n) = \text{Tr} \{ \rho E^-(x_1) \dots E^-(x_n) E^+(x'_1) \dots E^+(x'_n) \} \quad (101)$$

In the quantum case the order of the operators (annihilation and creation operators) is important.

The correlation function is a *normally ordered* function, i.e., all annihilation operators are on the right and all creation operators are on the left.

A few properties of the correlation function:

- $$G^{(1)}(x, x) = \text{Tr} \{ \rho E^-(x) E^+(x) \} \geq 0 \quad (102)$$

- $$G^{(1)}(x_1, x_1) G^{(1)}(x_2, x_2) \geq |G^{(1)}(x_1, x_2)|^2 \quad (103)$$

(Cauchy-Schwartz-inequality)

3.2 Optical Coherence

The first order correlation function (sometimes also amplitude correlation function) determines the degree of possible interference between two fields.

An interference can be measured, e.g., in a Young-type interference experiment (double slit experiment):

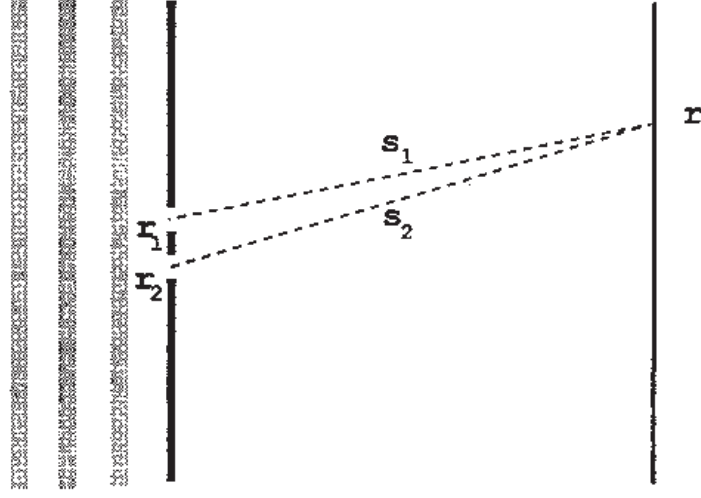


Figure 11: Principle of Young's double slit experiment [from Walls "Quantum Optics"]

At the point \vec{r} the field arises from a superposition of two (Huygens) elementary waves:

$$E^{(+)}(r, t) = E_1^{(+)}(r, t) + E_2^{(+)}(r, t) \quad (104)$$

with

$$E_i^{(+)}(r, t) = E_i^{(+)}(r_i, t - s_i/c) \frac{1}{s_i} e^{i(k-\omega/c)s_i} \quad (105)$$

where $s_i = |r_i - r|$.

Since $k - \omega/c = 0$ for a spherical wave it follows:

$$E^{(+)}(r, t) = \frac{E_1^{(+)}(r_1, t - s_1/c)}{s_1} + \frac{E_2^{(+)}(r_2, t - s_2/c)}{s_2} \quad (106)$$

$$\approx \frac{1}{R} [E^{(+)}(x_1) + E^{(+)}(x_2)] \quad (107)$$

where $R \simeq s_1 \simeq s_2$ and $x_i = (r_i, t - s_i/c)$.

Then

$$I(r) \propto Tr \{ \rho E^{(-)}(r, t) E^{(+)}(r, t) \} \quad (108)$$

$$= G^{(1)}(x_1, x_1) + G^{(1)}(x_2, x_2) + 2 \operatorname{Re} \{ G^{(1)}(x_1, x_2) \} \quad (109)$$

$$= G^{(1)}(x_1, x_1) + G^{(1)}(x_2, x_2) + 2 |G^{(1)}(x_1, x_2)| \cos \Psi(x_1, x_2) \quad (110)$$

where

$$G^{(1)}(x_1, x_2) = |G^{(1)}(x_1, x_2)| \exp(i\Psi(x_1, x_2)) \quad (111)$$

Interferenz fringes arise only if $G^{(1)}(x_1, x_2) \neq 0$!

One can define the normalized correlation function:

$$g^{(1)}(x_1, x_2) = \frac{G^{(1)}(x_1, x_2)}{[G^{(1)}(x_1, x_1)G^{(1)}(x_2, x_2)]^{1/2}} \quad (112)$$

The best fringe contrast in an interference experiment is obtained when

$$|G^{(1)}(x_1, x_2)| = [G^{(1)}(x_1, x_1)G^{(1)}(x_2, x_2)]^{1/2} \quad (113)$$

or

$$|g^{(1)}(x_1, x_2)| = 1 \quad (114)$$

$$\Leftrightarrow \quad (115)$$

$$g^{(1)}(x_1, x_2) = e^{i\Psi(x_1, x_2)} \quad (116)$$

The visibility v of fringes in an interference experiment is defined as:

$$v = \frac{I_{\max} - I_{\min}}{I_{\max} + I_{\min}} \quad (117)$$

$$= \left| \frac{G^{(1)}(x_1, x_2)}{[G^{(1)}(x_1, x_1)G^{(1)}(x_2, x_2)]^{1/2}} \right| \cdot \frac{2(I_1 I_2)^{1/2}}{I_1 + I_2} \quad (118)$$

$$= |g^{(1)}(x_1, x_2)| \cdot \frac{2(I_1 I_2)^{1/2}}{I_1 + I_2} \quad (119)$$

In the special case when $I_1 = I_2$:

$$v = |g^{(1)}(x_1, x_2)| \quad (120)$$

Obviously $|g^{(1)}(x_1, x_2)| = 1$ if $G^{(1)}(x_1, x_2)$ factorizes, i.e., if $G^{(1)}(x_1, x_2)$ can be written as

$$G^{(1)}(x_1, x_2) = \varepsilon^{(-)}(x_1)\varepsilon^{(+)}(x_2) \quad (121)$$

with some complex numbers ε .

Thus, a field is said to be fully coherent to n -th order if $G^{(n)}(x_1, x_2, \dots, x_n)$ factorizes.

This is the case if the state of the field is an eigenstate of the annihilation operator a .

Coherent states $|\alpha\rangle$ are coherent to all orders n .

What happens if the field is attenuated so much that only a single photon at a time passes through the double slit? Does the quantum nature of light effect the interference?

Such an experiment was performed by G.I. Taylor in 1909 (Interference fringes with feeble light, Proceedings of the Cambridge Philosophical Society 15 114-115).

In the quantum case the electric field at point \vec{r} is:

$$E^{(+)} = \sqrt{\frac{\hbar\omega}{\epsilon_0}} (u_1(r, t)a_1e^{ikr_1} + u_2(r, t)a_2e^{ikr_2}) \quad (122)$$

with

$$u_i(r, t) = \frac{\hat{\epsilon}_i}{(4\pi L)^{1/2}} \frac{1}{r} e^{-i\omega t} \quad (123)$$

The state of the single photon field after the Young slit is then:

$$|\psi\rangle = \frac{1}{\sqrt{2}}(a_1^+ + a_2^+) |0\rangle \quad (124)$$

It is then straightforward to show that

$$I(r, t) = \eta(1 + \cos \Phi) \quad (125)$$

with some amplitude η and phase Φ .

Thus, the result is the same as in the classical case. The probability amplitudes or the two paths of the single photon interfere like classical waves.

3.3 Photon Bunching and Antibunching

Whereas the first order coherence function $G^{(1)}$ describes *amplitude correlations*, the second order coherence function $G^{(2)}$ describes *intensity correlations*.

$$G^{(2)}(x_1, x_2) = \langle E^-(x_1)E^-(x_2)E^+(x_2)E^+(x_1) \rangle \quad (126)$$

$$= \text{Tr} (\rho E^-(x_1)E^-(x_2)E^+(x_2)E^+(x_1)) \quad (127)$$

$$= \langle : I(x_1)I(x_2) : \rangle \quad (128)$$

$$\propto \langle : n(x_1)n(x_2) : \rangle \quad (129)$$

The symbol $:$ denotes *normal ordering*.

A first application of the measurement of the first order coherence function was suggested by Michelson, the so-called **Michelson stellar interferometer**.

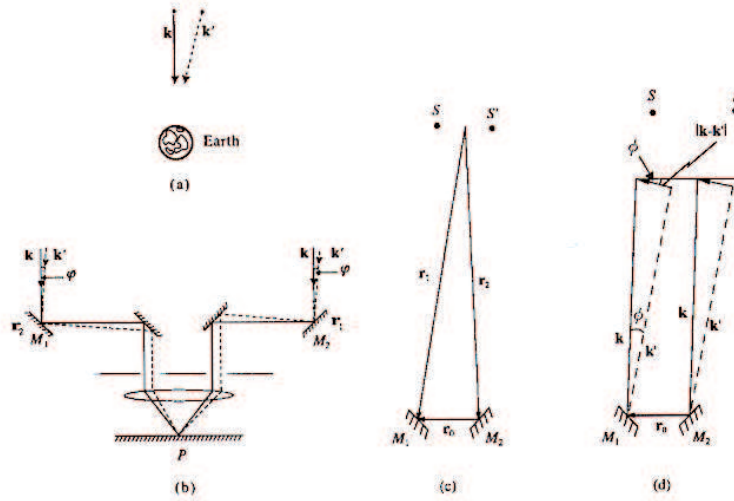


Figure 12: Principle of a Michelson stellar interferometer [from Scully "Quantum Optics"]

The interferometer can be used to determine the angular separation φ between two distant stars.

It is not too difficult to derive the Intensity $I(r_1 - r_2)$:

$$I(r_1 - r_2) = 4\kappa I_0 \left\{ 1 + \cos [(k + k')(r_1 - r_2)/2] \cos \left(\frac{\pi r_0 \varphi}{\lambda} \right) \right\} \quad (130)$$

where κ is some constant and λ is the wavelength of the radiation.

One difficulty, however, is that instrumental and atmospheric fluctuations very easily wash out the rapidly oscillating term $\cos [(k + k')(r_1 - r_2)/2]$.

A solution was suggested by Hanbury-Brown and Twiss, the **Hanbury-Brown and Twiss (HBT-) interferometer**.

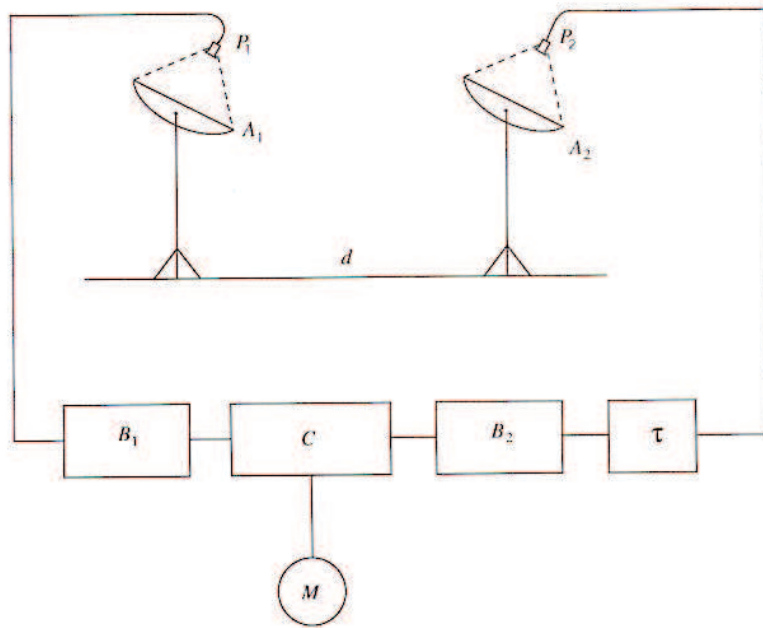


Figure 13: Principle of a HBT interferometer [from Scully "Quantum Optics"]

In this interferometer the intensities at two different positions (r_1 and r_2) are correlated:

$$I(r_i, t) = \kappa \left\{ |E_k|^2 + |E_{k'}|^2 + \left[E_k E_{k'} e^{i(k-k')r_i} + c.c \right] \right\} \quad (i = 1, 2)$$

and

$$\begin{aligned} \langle I(r_1, t)I(r_2, t) \rangle &= \kappa^2 \left\langle (|E_k|^2 + |E_{k'}|^2)^2 \right\rangle \\ &+ \kappa^2 \langle |E_k|^2 |E_{k'}|^2 \rangle \left[e^{i(k-k')(r_1-r_2)} + c.c. \right] \end{aligned} \quad (131)$$

The oscillating term is now much less sensitive to fluctuations (only the difference $k - k'$ enters!).

The normalized second order correlation function is given by:

$$g^{(2)}(x_1, x_2) = \frac{G^{(2)}(x_1, x_2)}{G^{(1)}(x_1, x_1)G^{(1)}(x_2, x_2)} \quad (132)$$

In the special case of temporal correlations at times t and $t + \tau$ one finds:

$$\begin{aligned} g^{(2)}(x_1, x_2) &= \frac{\langle E^-(t)E^-(t+\tau)E^+(t+\tau)E^+(t) \rangle}{\langle E^-(t)E^+(t) \rangle \langle E^-(t+\tau)E^+(t+\tau) \rangle} \\ &= \frac{\langle : I(t+\tau)I(t) : \rangle}{\langle : I(t) : \rangle \langle : I(t+\tau) : \rangle} \end{aligned} \quad (133)$$

For a second order coherent field:

$$G^{(2)}(\tau) = \varepsilon^{(-)}(t)\varepsilon^{(-)}(t+\tau)\varepsilon^{(+)}(t+\tau)\varepsilon^{(+)}(t) = (G^{(1)}(\tau))^2 \quad (134)$$

thus

$$g^{(2)}(0) = 1 \quad (135)$$

3.3.1 Some properties of $g^{(2)}$:

For classical fields the following properties follow from the Schwartz-inequality:

$$|\langle ab \rangle|^2 \leq \langle |a|^2 \rangle \langle |b|^2 \rangle \quad \text{for } a, b = c\text{-numbers} \quad (136)$$

Hence:

$$|\langle I(r, t)I(r, t+\tau) \rangle|^2 \leq \langle |I(r, t)|^2 \rangle \langle |I(r, t+\tau)|^2 \rangle \quad (137)$$

or:

$$g^{(2)}(\tau) \leq g^{(2)}(0) \quad \text{for classical fields} \quad (138)$$

The normalized second order coherence function for classical fields is constant or monotonously decreasing!

At times $\tau \geq 0$:

$$g^{(2)}(0) = 1 + \frac{\int P(\varepsilon) (|\varepsilon|^2 - \langle |\varepsilon|^2 \rangle)^2 d\varepsilon}{\langle |\varepsilon|^2 \rangle^2} \quad \text{for classical fields} \quad (139)$$

Since $P(\varepsilon)$ is a positive definite probability distribution is follows:

$$g^{(2)}(0) \geq 1 \quad \text{for classical fields} \quad (140)$$

The normalized second order coherence function for classical fields is larger than or equal to 1 at $\tau = 0$!

A classical fluctuating field may be regarded, e.g., as the sum of the fields from many atoms or molecules in a gas:

$$E(t) = \sum_i^v E_i(t) \quad \text{with} \quad \langle E_i(t) = 0 \rangle \quad (141)$$

Then:

$$G^{(2)}(t) = \langle E^*(t)E^*(t+\tau)E(t+\tau)E(t) \rangle \quad (142)$$

$$= \sum_{i=1}^v \langle E_i^*(t)E_i^*(t+\tau)E_i(t+\tau)E_i(t) \rangle \quad (143)$$

$$+ \sum_{i \neq j}^v \{ \langle E_i^*(t)E_j^*(t+\tau)E_j(t+\tau)E_i(t) \rangle + \quad (144)$$

$$\langle E_i^*(t)E_j^*(t+\tau)E_i(t+\tau)E_j(t) \rangle \} \quad (145)$$

Now only terms are retained where the field of each atom is multiplied by its complex conjugate. If all atoms are identical it follows:

$$G^{(2)}(t) = v \langle E_i^*(t)E_i^*(t+\tau)E_i(t+\tau)E_i(t) \rangle \quad (146)$$

$$= v(v-1) \{ \langle E_i^*(t)E_i(t) \rangle^2 + |\langle E_i^*(t)E_i(t+\tau) \rangle|^2 \} \quad (147)$$

For very large v the second term is much larger than the first. Thus:

$$G^{(2)}(t) \approx v^2 \{ \langle E_i^*(t)E_i(t) \rangle^2 + |\langle E_i^*(t)E_i(t+\tau) \rangle|^2 \} \quad (148)$$

and

$$g^{(2)}(t) = 1 + |g^{(1)}(t)|^2 \quad \text{for classical fields} \quad (149)$$

Hence, the spectrum $S(\omega)$ of a field is proportional to the Fourier transform of $G^{(1)}(t)$ it follows:

$$S(\omega) = \int_{-\infty}^{\infty} d\tau e^{-i\omega\tau} G^{(1)}(\tau) \quad (150)$$

Therefore, it holds:

$$g^{(2)}(\tau) = 1 + e^{-\gamma\tau} \quad \text{for a field with a Lorentzian spectrum} \quad (151)$$

$$g^{(2)}(\tau) = 1 + e^{-\gamma^2\tau^2} \quad \text{for a field with a Gaussian spectrum} \quad (152)$$

$$g^{(2)}(\tau) = 1 \quad \text{for a coherent field} \quad (153)$$

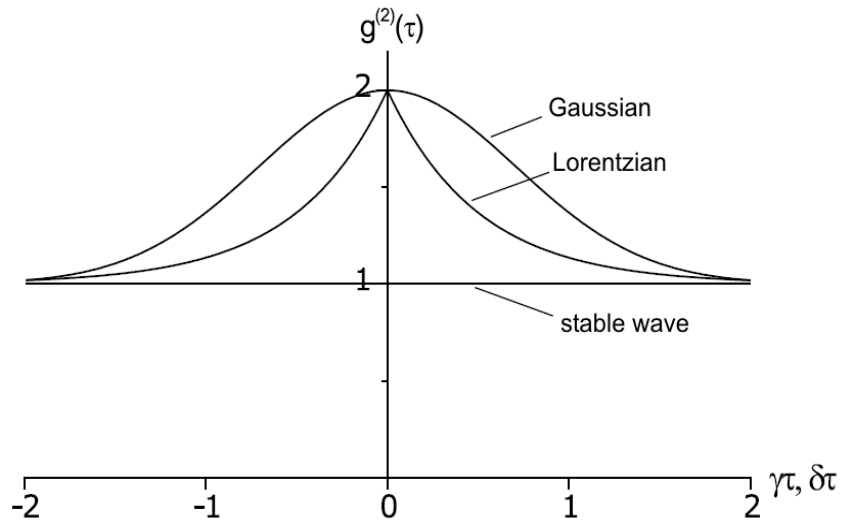


Figure 14: Normalized second order coherence functions for different fields

3.3.2 $g^{(2)}$ for quantum fields

For a single mode quantum field:

$$g^{(2)}(0) = \frac{\langle a^+ a^+ a a \rangle}{\langle a^+ a \rangle^2} = 1 + \frac{V(n) - \bar{n}}{\bar{n}^2} \quad (154)$$

where

$$V(n) = \langle (a^+ a)^2 \rangle - \langle a^+ a \rangle^2 \quad (155)$$

is the variance of the field.

Thus for a coherent (single mode) field $|\psi\rangle$ it is:

$$g^{(2)}(0) = 1 \quad (156)$$

and for a Fock state $|n\rangle$:

$$g^{(2)}(0) = 1 - \frac{1}{n} < 1 \quad (157)$$

The measurement of the intensity fluctuations shows directly if a field is a quantum field or a classical field!

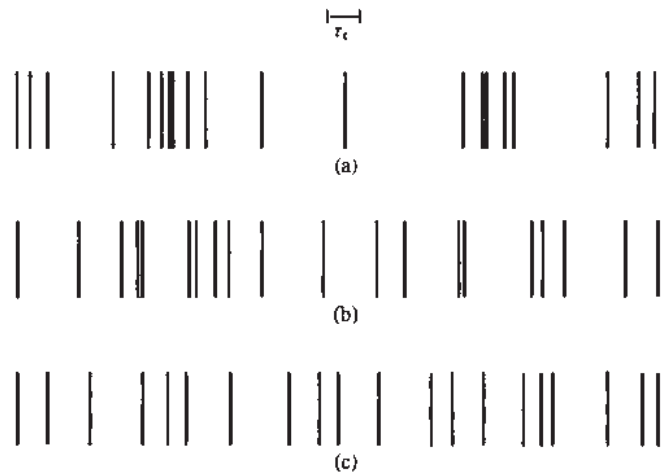


Figure 15: Photon count distribution (intensity fluctuation) for a thermal (top) coherent (middle) or quantum (bottom) field [from Scully "Quantum Optics"]

The three cases in the figure show **bunched light** ($g^{(2)}(0) > 1$) coherent light ($g^{(2)}(\tau) = 1$) and **anti-bunched light** ($g^{(2)}(\tau) < 1$).

In the limit $t \rightarrow \infty$ it is $g^{(2)}(\infty) = 1$.

3.4 Quantum Light

The question arises: How can one make quantum light?

Obviously, it is expected that light from a quantum source reveals its non-classical behaviour. Quantum light sources are, e.g.,

1. single atoms, molecules or ions,
2. single color defect centers,
3. single artificial atom,
4. or any source where light is coming from a transition between two distinct states.

First experiments with single atoms were realized in atomic beam experiments. Here, an atomic beam is attenuated so much, that only one or less than one atom on the average is measured.

The first experiment by Kimble et al., Phys. Rev. 39, 691 (1977) used a beam of sodium atoms and phototubes in single photon counting mode. The following pictures show the experimental setup (Fig 1 of the paper) and the experimental results (Fig 2 of the paper).

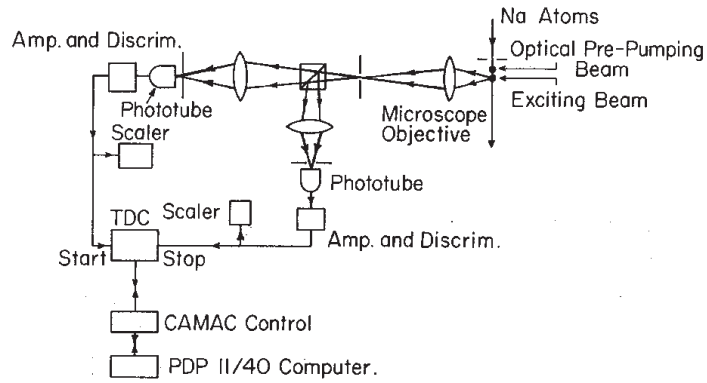


FIG. 1. Outline of the principal elements of the experiment.

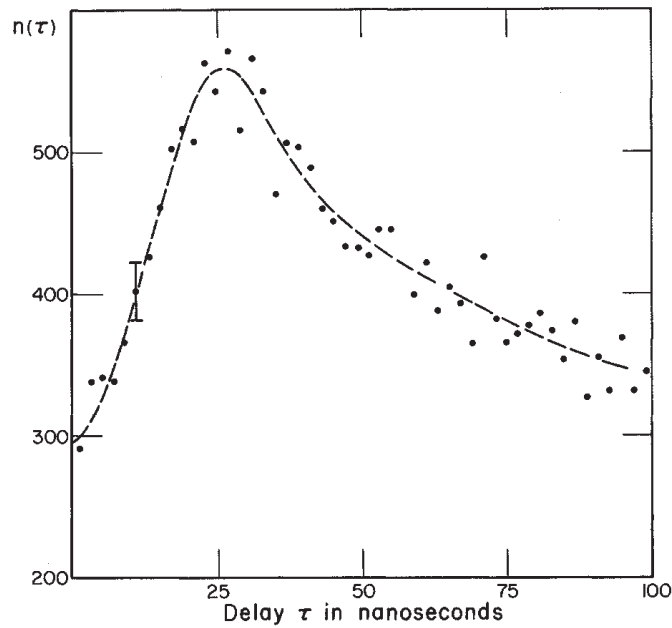


FIG. 2. The number of recorded pulse pairs $n(\tau)$ as a function of the time delay τ in nanoseconds. The growth of $n(\tau)$ from $\tau = 0$ shows antibunching. The bars on one point indicate statistical uncertainties corresponding to one standard deviation. The broken line just outlines the trend.

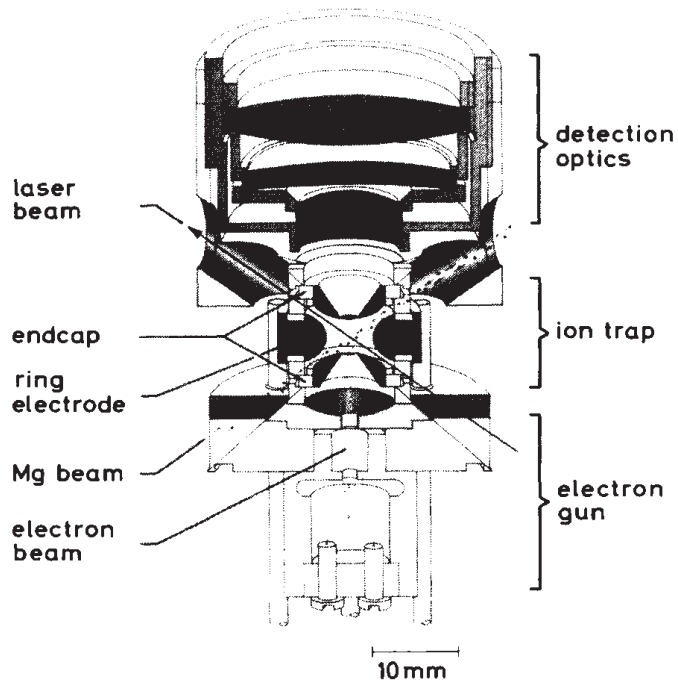


FIG. 1. Radio-frequency trap. The fluorescence light of the stored ion is observed through a bore in the upper pole cap.

Following experiments used single trapped ions or atoms. In an experiment by Dietrich and Walther, Phys. Rev. Lett. 58, 203 (1987) a single Mg-ion was trapped in a Paul-trap and its fluorescence light was detected.

The picture above shows the experimental setup (Fig 1 of the paper) and the picture below shows the experimental results (Fig 3 of the paper).

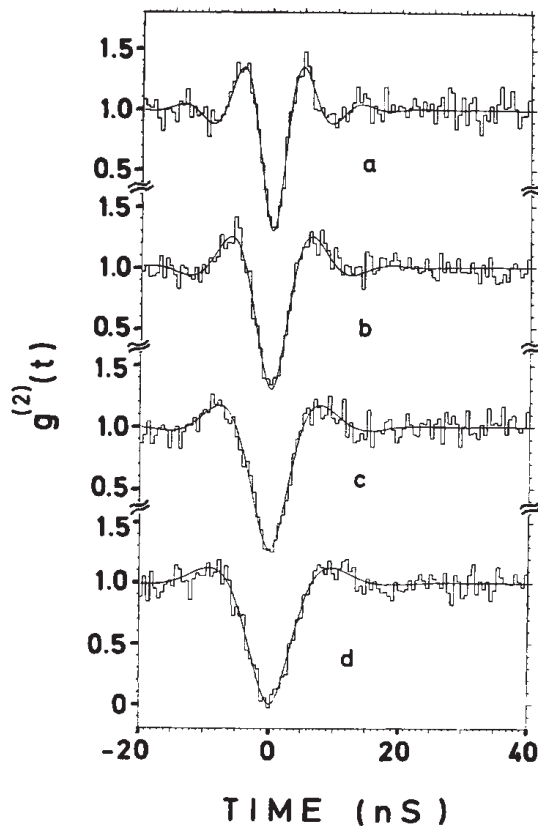


FIG. 3. Antibunching signal of a single ion for different laser intensities. The data have been corrected for the micro-motion of the ion; in addition, the background due to accidental coincidences was subtracted.

Anti-bunched light can be used to realize single photon sources, which will be needed in novel technologies such as quantum cryptography and all-optical quantum computing.

3.5 Single Photon Sources

The most fundamental light source is an emitter of single photons. In the last decade several realizations of such sources have been demonstrated.

One possibility to make is single photon source is to excite a single quantum system. If the main path of relaxation from the excited state is radiative decay, then only

a single photon is emitted at a time. A possible system is a single atom or ion as demonstrated in the previous section. However, any system with a discrete energy level structure can be utilized. Examples are:

- atoms/ions
- molecules
- color centers (e.g. defect centers in diamond)
- zero-dimensional semiconductor nanostructures (quantum dots)

In quantum dots electrons and holes are confined within a potential formed by a semiconductor heterostructure. If the localization is tight enough (typically within a few nanometers) then the charge carriers show a pronounced discretization of allowed energy states. Recombination of single electrons and single holes produces discrete spectral lines, similar as in atoms.

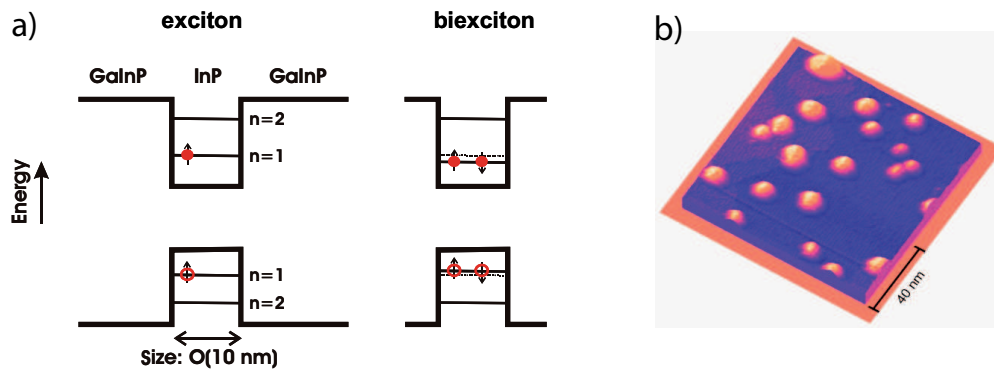


Figure 16: a): Schematics of bandgap structure of a quantum dot (GaInP/InP heterostructure). Configurations with a single electron-hole pair (exciton state) and with two electron-hole pairs (biexciton state) are shown. b): AFM image of several quantum dots.

Figure 16 shows a schematics of the energy bands in a quantum dot heterostructure together with an AFM-image of a single InP quantum dot.

Quantum dots can be fabricated with semiconductor growth technology. They further offer the advantages of stability and the possibility of both optical and electrical excitation. Presently, single photon sources based on quantum dots are developed as quantum optical devices for non-classical light.

Figure 17 shows the measured $g^{(2)}$ -function of fluorescence light from a single optically excited quantum dot under continuous (cw) and pulsed excitation.

The experimental results agree very well with the theoretically expected curves shown in Fig. 18.

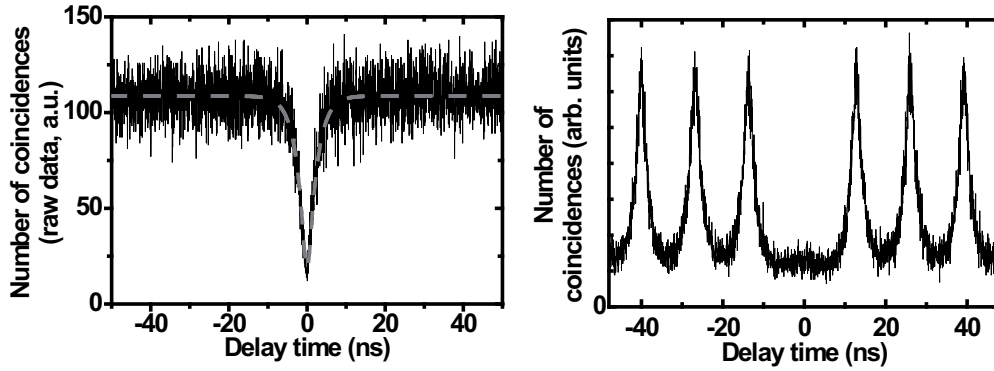


Figure 17: Measured $g^{(2)}$ -function of fluorescence light from a single optically excited quantum dot under continuous (left) and pulsed (right) excitation.

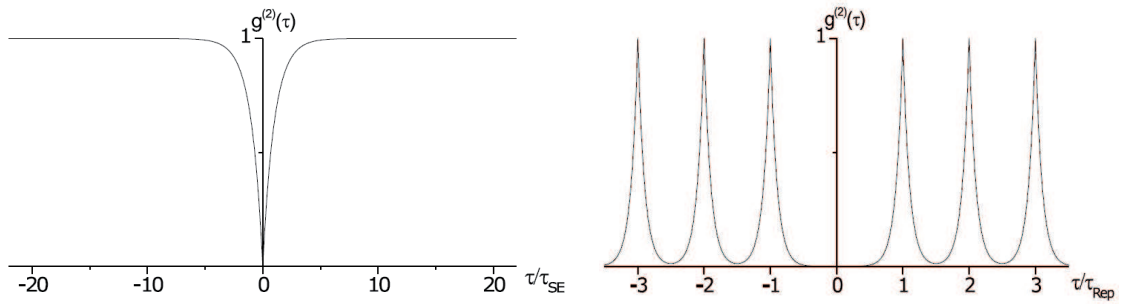


Figure 18: Theoretical $g^{(2)}$ -function of light from a single quantum emitter under continuous (left) and pulsed (right) excitation.